

# Characterisation of Passivated Aluminium Nanopowders: An XPS and TEM/EELS Study

J. C. Sánchez-López,\* A. Caballero and A. Fernández

Instituto de Ciencia de Materiales de Sevilla and Departamento Química Inorgánica, Centro de Investigaciones Científicas 'Isla de la Cartuja', Avda. Americo Vespuccio s/n, 41092 Sevilla, Spain

## Abstract

*We present here, an exhaustive characterisation of an ultrafine  $Al_2O_3/Al$  powder prepared by passivation with oxygen of aluminium nanopowders. By compaction and sintering of this material, a nanostructured  $Al_2O_3/Al$  foil with singular properties has been prepared. Actually, the powdered precursor material is formed by metallic Al cores covered by an alumina passivation layer. Transmission electron microscopy (TEM) shows the presence of small grains with a mean particle size of ca 23 nm and a high degree of coalescence between grains. X-ray photoelectron spectroscopy (XPS) studies show the formation of an alumina passivation layer with a thickness of around 4 nm which prevents the material from further oxidation. However, this technique does not make important differences between a geometry of isolated spherical particles and the real situation of interconnected grains. Another characterisation technique that we have used is the electron energy loss spectroscopy (EELS) in a transmission electron microscope. By this technique, the Al K edge excitation spectrum can be recorded in a similar way to that recorded by X-ray absorption spectroscopy (XAS) measurements. From the electron loss near edge structure (ELNES), we could predict the coalescence of the nanoparticles in the powdered sample. An average particle aggregation number of 4 was estimated to get the best reproduction of the experimental data. These results are in good concordance with TEM observations. © 1998 Elsevier Science Limited. All rights reserved*

## 1 Introduction

Nanocrystalline or nanostructured ultrafine powders (grain size below 50 nm) have attracted considerable attention in the last few years because of their unique characteristics that cannot be obtained in the conventional powders.<sup>1</sup> The chemical and structural characterisation of such ultrafine powders is at this respect an important field of research. In the present paper we describe the use of the X-ray photoelectron spectroscopy (XPS) and the electron energy loss spectroscopy (EELS) in a transmission electron microscope to characterise such nanostructured powders.

In particular, we have studied Al nanopowders that have been prepared by the inert gas evaporation technique.<sup>2</sup> Al was evaporated in an  $N_2$  atmosphere and the ultrafine powder, collected on a cold finger, was passivated with oxygen before opening the chamber to air. Under these conditions the obtained material is made of particles of metallic aluminium covered by a very thin alumina overlayer. By compaction and sintering of this material we could prepare a nanostructured Al-oxide/Al foil that, although showing metallic shine and low ohmic resistivity, can be heated up to temperatures as high as 1000°C without breaking its structure.<sup>3</sup> It has been also shown that this nanocomposite is a low density high strength material.<sup>4</sup>

In the present paper we have used a surface analysis technique, the XPS, to characterise the alumina passivation overlayer. By analysis of the photoelectron spectra of Al and O, conclusions about the passivation mechanism of this material could be obtained.

Complementary information has also been obtained by EELS. This technique carried out in a

\*To whom correspondence should be addressed. e-mail: JCLOPEZ@cica.es

transmission electron microscope becomes a bulk analysis technique.<sup>5</sup> The electron loss near edge structure (ELNES) region of the EELS spectra may provide chemical and structural information in an analogous way to the X-ray absorption near edge structure (XANES)<sup>6</sup> spectra. The application of this technique to the study of passivated aluminium nanopowders will be described in the present work.

Finally, it is important to emphasise that the procedure described here may have applications to solve other problems during characterisation of nanostructured materials. In particular, we have previously reported the characterisation of this type of samples by XPS.<sup>3</sup> In the present paper we describe a comparative and complementary study using XPS and EELS techniques to analyse the same sample.

## 2 Experimental

The experimental device used for the synthesis of the Al ultrafine grains<sup>2,3</sup> consists of a small HV chamber pumped to a residual vacuum better than  $5 \times 10^{-7}$  Torr. A tungsten boat, containing small pieces of an Al foil (from Goodfellow metals 99.0% pure), was heated resistively up to a temperature of 1350°C in an N<sub>2</sub> atmosphere of  $\sim 1$  Torr. The evaporated material loses kinetic energy by collisions with the gas molecules and condenses as small particles that were collected on a cold finger. After preparation, the chamber was evacuated and the powder was passivated by introducing small doses of oxygen before exposure to air. The loose powder was then smoothly stripped off and stored in air. We will name this sample hereafter as Al<sub>2</sub>O<sub>3</sub>/Al-nano. An Al foil and an Al<sub>2</sub>O<sub>3</sub> sample obtained by thermal oxidation of aluminium were used as references.

TEM examination of the sample was carried out in a Philips CM10 microscope working at 100 kV. The samples were dispersed in ethanol by sonication and dropped on a copper grid coated with a holed carbon film. Particle size distribution was evaluated from several micrographs using an automatic image analyser. The number of particles selected for consideration in the statistical calculus was 425. The particle size is defined as 2 times the average radius measured from the center of area to the perimeter of the particle.

XRD analysis was carried out using CuK<sub>α</sub> radiation in a Siemens D5000 diffractometer.

X-ray photoelectron spectroscopy (XPS) spectra were recorded in a VG-Escalab 210 spectrometer working in the constant analyser energy mode with a pass energy of 50 eV and using MgK<sub>α</sub> radiation

as excitation source. The binding energy (BE) reference was taken at the C1s peak from carbon contamination of the samples at 284.5 eV. An estimated error of  $\pm 0.1$  eV can be assumed for all measurements. For quantification, the XPS spectra were subjected to background subtraction (Shirley background).<sup>7</sup> Data fit was carried out by a least squares routine supplied by the instrument manufacturer, using Gaussian–Lorentzian peaks.

Two models have been used to calculate the expected surface elemental composition to be measured by XPS for this type of samples. Firstly, we used the model of Sheng and Sutherland<sup>8</sup> for spherically shaped powders of small size ( $< 1 \mu\text{m}$ ) coated with a uniform overlayer [see Fig. 1 (a), isolated spheres model]. In this model, the angular and radial dependence of the pathlength of the photoelectrons generated within the substrate and the overlayer has been taken into account, as well as the difference in photoelectron inelastic mean free path (IMFP) between the substrate and the overlayer.<sup>8</sup> We assumed a spherical particle of metallic aluminium (density:  $2.7 \text{ g cm}^{-3}$ ) coated with a passivation layer of Al<sub>2</sub>O<sub>3</sub> (density assumed to be  $3.9 \text{ g cm}^{-3}$ ) and calculated the expected percentages of Al<sup>3+</sup> to be measured by XPS for different overlayer thickness. Nevertheless, as the transmission electron micrograph of the samples showed a high degree of interconnection and coalescence between grains, a second model has been used, consisting of a layer of Al<sup>0</sup> between two Al<sub>2</sub>O<sub>3</sub> thin layers [see Fig. 1(b), continuous layered model]. The exponential decay in intensity of the emitted photoelectrons<sup>9</sup> is given by

$$I = I_0 \cdot \exp(-x/\lambda)$$

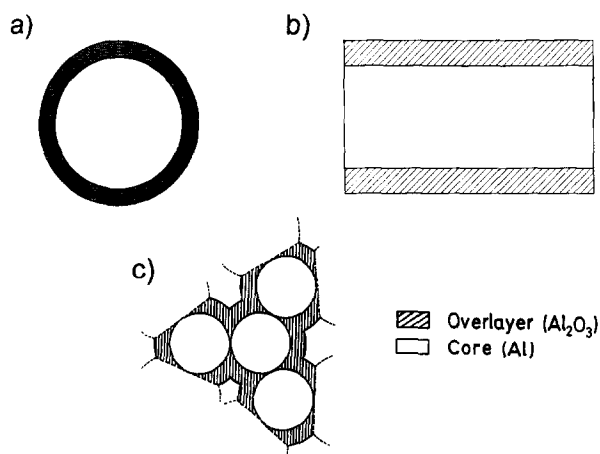


Fig. 1. Cross-section view of the used models simulating the sample morphology: (a) isolated spherical particles of Al<sup>0</sup> covered by an Al<sub>2</sub>O<sub>3</sub> overlayer (isolated spheres model); (b) a layer of Al<sup>0</sup> between two Al<sub>2</sub>O<sub>3</sub> thin layers (continuous layered model); (c) cluster of four spherical Al<sup>0</sup> particles covered by an Al<sub>2</sub>O<sub>3</sub> overlayer (coalescent model).

where  $x$  is the displacement of the electron from its point of origin and  $\lambda$  is the corresponding IMFP. The integration of this function for the continuous layered model considering different  $\text{Al}_2\text{O}_3$  overlayer thickness leads to the curves discussed below. IMFPs of the  $\text{Al}2p$  photoelectrons in the alumina overlayer and in the aluminium substrate were calculated using the empirical equations of Seah and Dench.<sup>9</sup> They were found to be 33 and 18.5 Å, respectively.

EELS spectra have been acquired in a Philips EM 420 microscope operating at 120 kV and fitted with a Gatan model 666 parallel detection electron spectrometer. In order to record the Al K-edge, the illuminated area was approximately 1  $\mu\text{m}$  in diameter and the integration time in the photo-diode array was 6 s. Spectra were recorded in the diffraction mode with a camera length of 122 mm and a collection angle of 15 mrad. No condense aperture and an EELS entrance aperture of 5 mm were used to increase the signal. Although no specific study of radiation damage was performed, it was visually checked that during the experiment the specimen did not evolve. The measured energy resolution of the coupled microscope/spectrometer system was about 1.5 eV. The expected amounts of  $\text{Al}_2\text{O}_3$  and  $\text{Al}^0$  phases to be detected by EELS can be calculated attending to the bulk analysis character of this technique. The atomic percentages of

$\text{Al}^{3+}$  and  $\text{Al}^0$  are determined for each model considering the geometry of the system and the densities for alumina and metallic aluminium. Together with the two models described above for the XPS calculations, another model has been used in the case of EELS that consists of the coalescence of a cluster of four interconnected spherical  $\text{Al}^0$  particles, covered by an  $\text{Al}_2\text{O}_3$  overlayer [see Fig. 1(c), coalescent model].

### 3 Results

Figure 2 shows a TEM micrograph and the particle size distribution histogram of the  $\text{Al}_2\text{O}_3/\text{Al}$ -nano sample. Particles size ranging from 10 to 40 nm and a mean particle size of 23 nm have been determined for this sample. It can be also noticed the high degree of interconnection or coalescence between grains. The measurements of crystallite size is referred to the particles that remain identifiable within the agglomerates.

The XRD diffractogram of the passivated Al nanoparticles (Fig. 3, top) indicates the presence of pure metallic aluminium. The  $\text{Al}2p$  photoelectron spectrum of the sample (Fig. 3, bottom) shows, however, that most of the aluminium on the surface is oxidised to  $\text{Al}^{3+}$  species. In fact, due to the preparation procedure the sample is made up

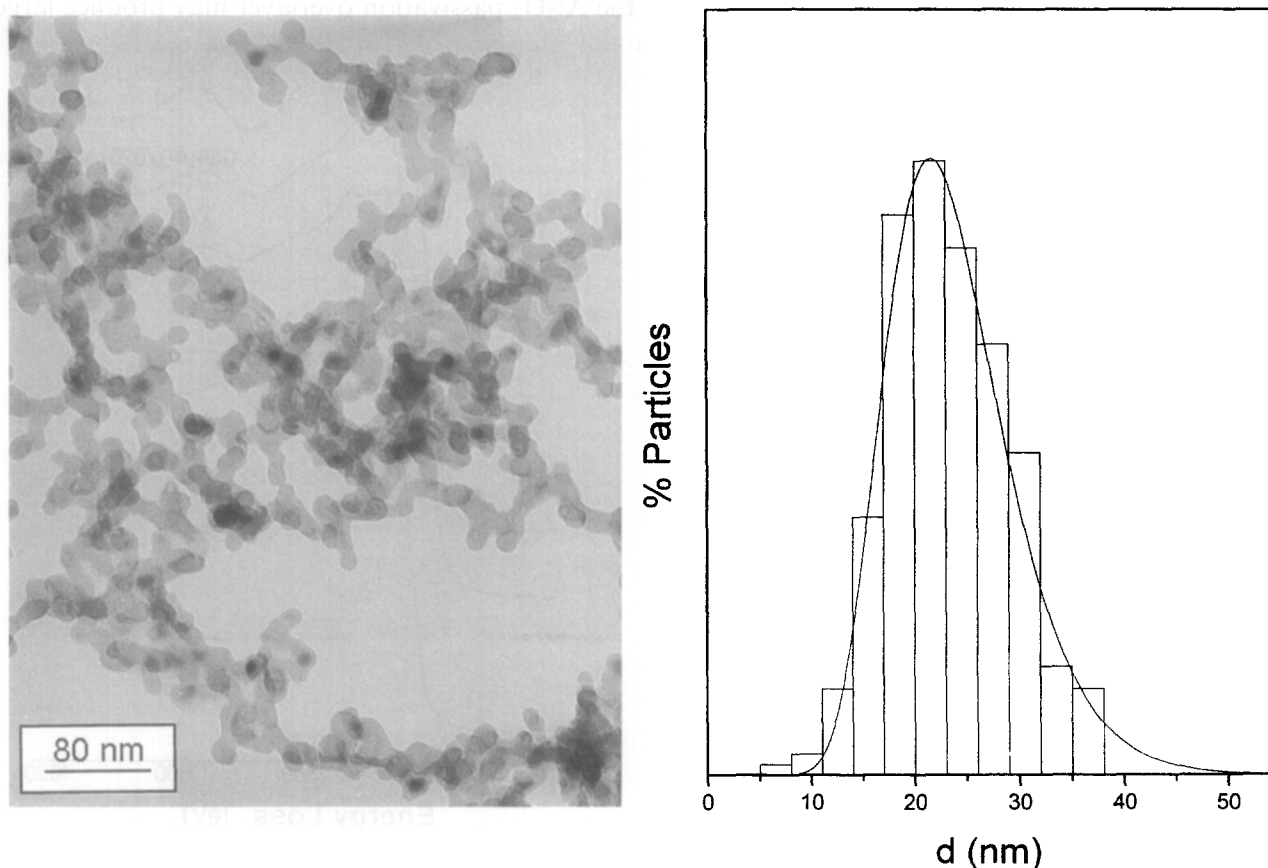


Fig. 2. TEM micrograph (left) and particle size distribution histogram (right) for the  $\text{Al}_2\text{O}_3/\text{Al}$ -nano sample. Superimposed on the histogram is the log-normal distribution function.

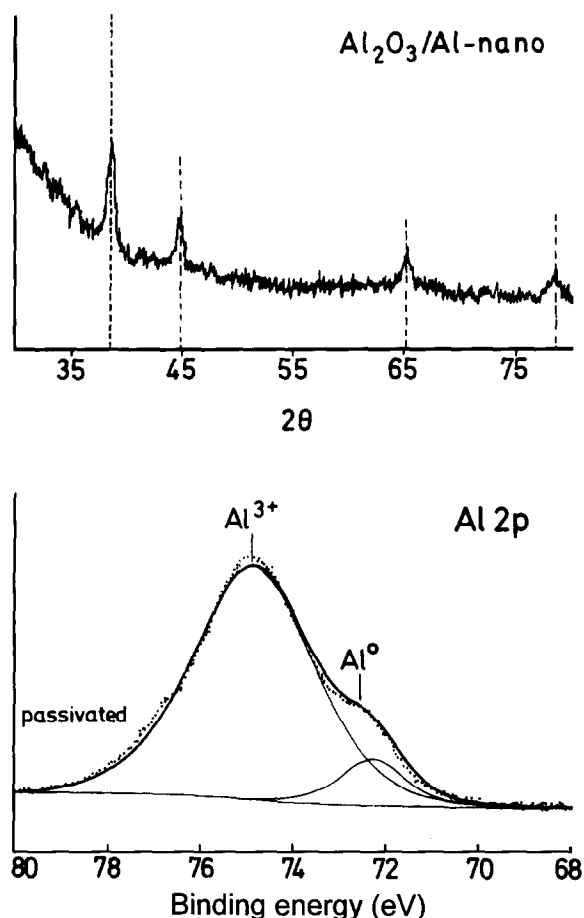


Fig. 3. XRD diffraction pattern (top) and Al2p photoelectron spectrum (bottom) of the Al<sub>2</sub>O<sub>3</sub>/Al-nano sample. Dashed lines in the top figure represent the diffraction peaks from metallic fcc aluminium.

of aluminium metallic cores coated by an alumina overlayer. This Al<sub>2</sub>O<sub>3</sub> passivation layer is very thin and it is not well crystallised so that XRD peaks from Al<sub>2</sub>O<sub>3</sub> could not be detected. The fitting analysis of the Al2p photoelectron spectrum in terms of Al<sup>0</sup> and Al<sup>3+</sup> components is also shown in Fig. 3 (bottom). This analysis enabled us to evaluate the percentage of oxidised Al<sup>3+</sup> and Al<sup>0</sup> species in the total aluminium signal being obtained values of 89 and 11%, respectively. It is worth of mention that the oxidation of the aluminium nanoparticles progress to achieve a steady-state situation in which the amount of Al<sup>3+</sup> detected by XPS does not increase. These results are in agreement with the well established behaviour of microcrystalline aluminium which, during oxidation by air exposure, produces a dense and compact passivation Al<sub>2</sub>O<sub>3</sub> overlayer that avoid the progressive oxidation of the material.<sup>10</sup>

Figure 4 shows the near edge structure of the EELS spectra (ELNES) obtained in the transmission electron microscope for the Al<sub>2</sub>O<sub>3</sub>/Al-nano sample as compared to that of an Al foil and an alumina reference sample. The feature of the ELNES spectra contains information about the type of short range structure in an analogous way

to the XANES region of the XAS spectra.<sup>11</sup> Although the simulation of the ELNES spectra is complicated one can use this as a fingerprint technique. In this case we have carried out a linear combination of the reference spectra for the Al and Al<sub>2</sub>O<sub>3</sub> to get the best reproduction of the experimental ELNES spectrum for the nanocrystalline Al<sub>2</sub>O<sub>3</sub>/Al-nano sample. These results are summarised in Fig. 4 giving a value of 35% of Al in the form of Al<sub>2</sub>O<sub>3</sub> and 65% of metallic Al. In the following paragraphs we describe the use of the models introduced in the experimental part to evaluate the Al<sup>3+</sup> and Al<sup>0</sup> atomic percentages to be measured by both techniques, XPS and EELS. These calculations will allow us to obtain information about the thickness of the alumina passivation layer and the average aggregation degree of the nanostructured Al<sub>2</sub>O<sub>3</sub>/Al powder.

Figure 5(A) shows the calculated percentage of Al<sup>3+</sup> to be detected by XPS for the isolated spheres and continuous layered models as a function of the thickness of the alumina overlayer. Al<sup>0</sup> spherical particles of 15 nm in diameter and an Al<sup>0</sup> layer of 15 nm have been considered for calculations. Similar curves were found for Al<sup>0</sup> core sizes ranging from 15 to 30 nm. In fact, due to the surface analysis character of the XPS, the curves are more influenced by the Al<sub>2</sub>O<sub>3</sub> overlayer thickness than the particle size. Small changes in the thickness of the Al<sub>2</sub>O<sub>3</sub> passivation overlayer may produce large

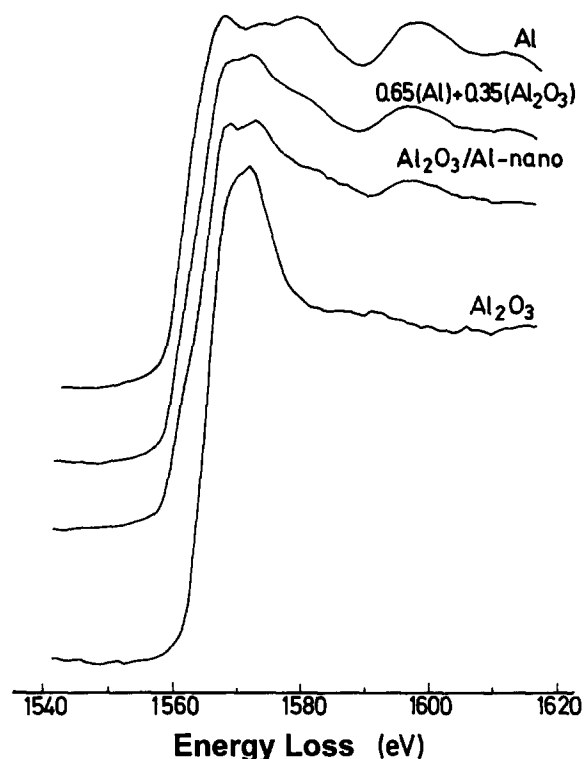


Fig. 4. ELNES spectra at the Al K-edge for the Al<sub>2</sub>O<sub>3</sub>/Al-nano sample in comparison to Al and Al<sub>2</sub>O<sub>3</sub> references. A calculated (best fit) spectrum obtained by linear combination of the reference spectra is also included.

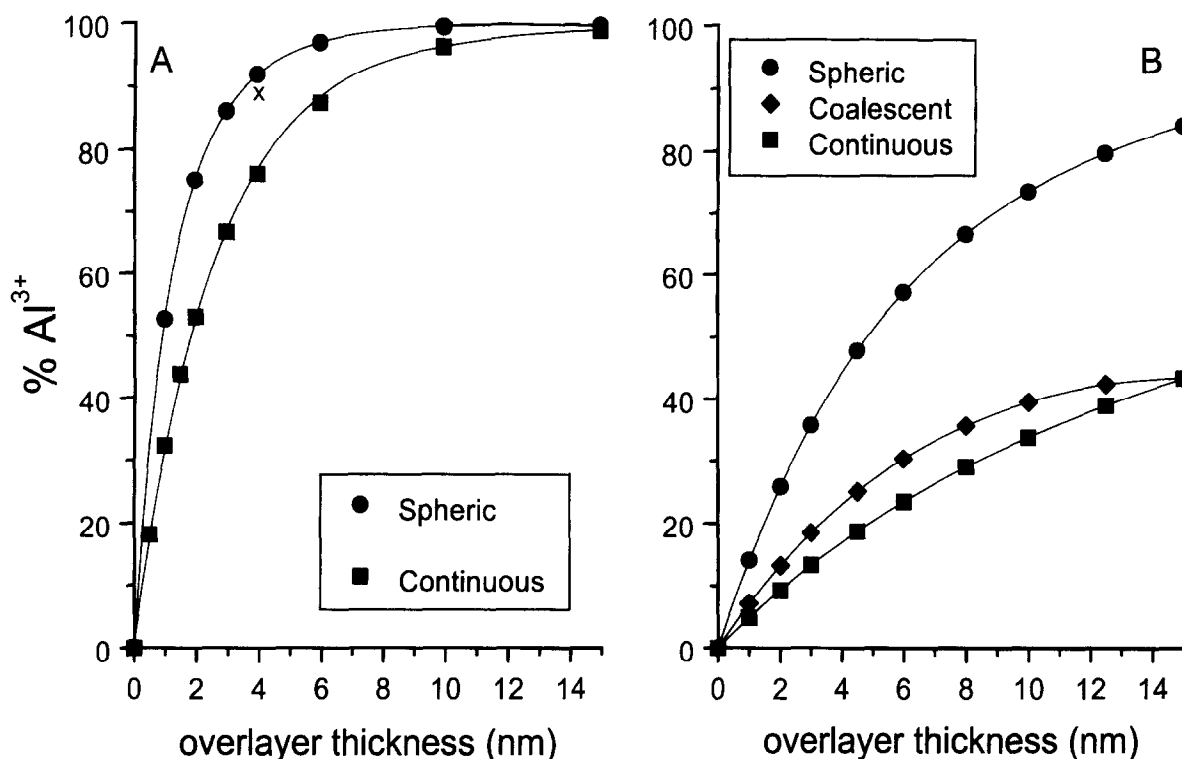


Fig. 5. (A) Effects of alumina overlayer thickness on calculated Al<sup>3+</sup> percentages to be measured by XPS for the (a) isolated spheres and (b) continuous models; (B) effects of alumina overlayer thickness on calculated Al<sup>3+</sup> percentages to be measured by EELS for the (a) isolated spheres, (b) continuous and (c) coalescent models. (Al<sup>0</sup> spherical particles of 15 nm in diameter and an Al<sup>0</sup> layer of 15 nm have been considered for calculations).

changes in the percentages of Al<sup>3+</sup> detected by XPS for very thin alumina overlayers. The experimental value of Al<sup>3+</sup> obtained from the XPS analysis of the sample is 89% after steady-state passivation. This situation is indicated by a cross in Fig. 5(A) for an intermediate curve between the one of isolated spheres and the continuous model. For this value, the thickness of the Al<sub>2</sub>O<sub>3</sub> coating layer can be estimated to be ca 4 nm what leads to a total particle size for the passivated particles of 23 nm. In addition, the value of 4 nm outlined here is between previously reported values of 2 nm, as measured by HRTEM,<sup>12</sup> and 6 nm obtained from energy filtered images<sup>13</sup> of nanostructured aluminium particles. A similar study carried out with samples of different total particles sizes ranging from 12 to 41 nm shows a constant value for the thickness of the alumina overlayer of 4 nm. These results are in agreement with the well known behaviour of aluminium<sup>10</sup> in which oxidation progresses to form a dense and compact passivation Al<sub>2</sub>O<sub>3</sub> overlayer that protects the material from further oxidation. This type of overlayer is also formed on nanostructured aluminium, opening a route of preparation of an Al<sub>2</sub>O<sub>3</sub>/Al nanocomposite materials with singular properties.<sup>3,4,14</sup>

In Fig. 5(B) we have presented the expected Al<sup>3+</sup> percentages to be detected by EELS for the three models described in the experimental part and depicted in Fig. 1. It is important to emphasise that

apart from changes in the detected Al<sup>3+</sup> percentages due to variation in overlayer thickness, important variations (up to 50%) can be observed by changing the morphology of the powdered sample. For a size of aluminium core of 15 nm and for an Al<sub>2</sub>O<sub>3</sub> overlayer of 4 nm the values predicted from Fig. 5(B) are as follows: 66.5% of Al as Al<sub>2</sub>O<sub>3</sub> and 33.5% as Al<sup>0</sup> for the isolated spheres model, 29% of Al as Al<sub>2</sub>O<sub>3</sub> and 71% as Al<sup>0</sup> for the continuous layered model and 36% of Al as Al<sub>2</sub>O<sub>3</sub> and 64% as Al<sup>0</sup> for the coalescent model. The agreement of the values obtained for a cluster of four particles with the experimental data obtained from the ELNES linear combination is in good concordance with the TEM observed morphology of the powdered sample. Similar calculations carried out on clusters of two or three particles did not produce good fit to the experimental data.

#### 4 Conclusions

In the present paper we describe a comparative and complementary study by using XPS and EELS analysis of passivated aluminium nanopowders. Several conclusions have been obtained:

1. We have found a universal behaviour during passivation of Al nanocrystalline particles by air exposure as stated by XPS analysis. The

alumina overlayer achieves a steady-state thickness of ca 4 nm what allows the controlled preparation of Al<sub>2</sub>O<sub>3</sub>/Al nanocomposite materials with interesting properties. The XPS technique appears to be very sensitive to changes in the thickness of the Al<sub>2</sub>O<sub>3</sub> overlayer but not to textural changes of the powdered sample.

2. The EELS analysis appears to be sensitive both to the thickness of the alumina overlayer and the texture of the sample. The EELS results described in the present work show clearly that the powdered Al<sub>2</sub>O<sub>3</sub>/Al-nano sample is formed by spherical grains with a high degree of coalescence and not by isolated spherical particles. An average particle aggregation of four has been estimated from this study.
3. We have shown that XPS and EELS can provide complementary and valuable information for the characterisation of nanostructured materials and in particular for nanoparticles coated by an overlayer. XPS, as a surface analysis technique, provides information on the thickness and chemical composition of surface layers. The EELS at the transmission electron microscope is a bulk analysis technique that provides information on the texture of the materials and specially on the short range structure of nanostructured materials

#### Acknowledgements

The authors thank the DGICYT (project nos PB93-0183 and PB96-0863-C02-02) and 'Fundación Domingo Martínez' for financial support.

#### References

1. (a) Gleiter, H., Materials with ultrafine microstructures: retrospectives and perspectives. *Nanostruct. Mater.*, 1992, **1**, 1–19; (b) Siegel, R. W., Nanostructured materials—mind over matter. *Nanostruct. Mater.*, 1994, **4**, 121–138; (c) Gleiter, H., Nanostructured materials. State of the art and perspectives. *Nanostruct. Mater.*, 1995, **6**, 3–14.
2. Gleiter, H., Nanostructured materials. *Adv. Mat.*, 1992, **4**, 474–481.
3. Sánchez-López, J. C., Fernández, A., Conde, C. F., Conde, A., Morant, C. and Sanz, J. M., The melting behavior of passivated nanocrystalline aluminum. *Nanostruct. Mater.*, 1996, **7**, 813–822.
4. Suits, B. H., Apte, P., Wilken, D. E. and Siegel, R. W., NMR study of nanophase Al/Al-oxide powder and consolidated composites. *Nanostruct. Mater.*, 1995, **6**, 609–612.
5. Egerton, R. F., *Electron Energy-Loss Spectroscopy in the Electron Microscope*. Plenum Press, New York, 1986.
6. Schaich, W. L., Derivation of single-scattering formulas for X-ray absorption and high-energy electron-loss spectroscopies. *Phys. Rev. B*, 1984, **29**, 6513–6519.
7. Briggs, D. and Seah, M. P., *Practical Surface Analysis by Auger and X-Ray Photoelectron Spectroscopy*. John Wiley & Sons, Chichester, UK, 1990, pp. 233–236.
8. Sheng, E. and Sutherland, I., A quantitative XPS study of spherically shaped powders coated with an overlayer. *Surf. Sci.*, 1994, **314**, 325–330.
9. Seah, M. P. and Dench, W. A., Quantitative electron spectroscopy of surfaces: a standard data base for electron inelastic mean free path in solids. *Surf. Int. Anal.*, 1979, **1**, 1–11.
10. Cabrera, N. and Mott, N. F., Theory of the oxidation of metals. *Rept. Progress Phys.*, 1949, **12**, 163–814.
11. Koningsberger, D. C. and Prins, R., X-ray absorption. Principles, applications, techniques of EXAFS, SEXAFS and XANES. John Wiley & Sons, New York, 1988.
12. Sun, X. K., Xu, J., Chen, W. X. and Dei, W. D., Preparation of Al nanoparticles in a controlled environment. *Nanostruct. Mater.*, 1994, **4**, 337–344.
13. Eckert, J., Holzer, J. C., Ahn, C. C., Fu, Z. and Johnson, W. L., Melting behavior of nanocrystalline aluminum powder. *Nanostruct. Mater.*, 1993, **2**, 407–413.
14. Sánchez-López, J. C., Gonzalez-Elipe, D. E. and Fernández, A., Passivation of nanocrystalline Al prepared by the gas phase condensation method: An x-ray photoelectronspectroscopy study. *J. Mater. Res.*, 198, **13**, 703–710.